

A model of sediment transport over an intertidal transect, comparing the influences of biological and physical factors

Rose Wood and John Widdows

Plymouth Marine Laboratory, Prospect Place, West Hoe, Plymouth, PL1 3DH England

Abstract

This paper compares modeled biotic and physical effects on intertidal sediment transport, using parameterizations that are based on laboratory and field experiments. A one-dimensional model of an intertidal transect is constructed. The model is aligned cross shore and includes movement of water and suspended sediment. Within the model, tidal currents cause erosion, and bioturbation by the clam, *Macoma balthica*, alters the erodability of the bed sediment. The concentration of chlorophyll *a* in the surface sediment (which is an indicator of microphytobenthos density) alters the critical erosion velocity. External sediment supply is specified as an offshore suspended matter concentration. The model is applied within Spurn Bight (Humber Estuary, UK). The effects of various tide heights, biota densities, and external suspended sediment concentrations are investigated. Offshore sediment supply dominates the net deposition below midtide level, but factors affecting intertidal sediment erosion and deposition become important at higher shore levels. Changes in erosion or deposition caused by natural variation in biota densities are as large as those caused by changes in tidal range and currents over a spring–neap cycle, or by doubling external supply. Seasonal variations in densities of stabilizing microphytobenthos can alter the magnitude of net deposition on the upper shore by a factor of two. Interannual variation in numbers of bioturbating clams can change net deposition by a factor of five. These results show that biotic influences on transport of sediment within the intertidal zone are significant and will play a role in determining sediment budgets over tidal to monthly timescales.

Sheltered estuaries often have extensive intertidal areas. These are important as both sources and sinks for fine sediment within the estuary. As such, they have a major role in the storage and cycling of those pollutants that preferentially bind to small particles. Mudflats and salt marshes in the U.K. are an important habitat for wintering birds and their prey species. Accretion of mudflats and salt marshes provides a valuable natural coastal defense in a regime of rising sea level, serving to dissipate energy from high tides and storm waves.

The shallow coverage of water on the intertidal zones allows wave energy to penetrate to the bed, increasing the effect of small waves on sediment erosion. Rapid tidal flooding and drying of large, low gradient areas can also cause erosion by raising current speeds above the critical value. Turbid water is advected across the flats as the tide rises and is deposited during the long period of low current speeds near high water. Populations of benthic animals can affect erosion and deposition of particles actively (through bioturbation and biodeposition) and passively (by altering sediment characteristics). Algal mats and macroalgae can physically shield sediment, alter cohesiveness, and influence current velocity profiles.

This paper addresses the question of how important biotic effects on sediment transport over a whole tidal cycle are compared to the importance of tidal forcing and external sediment supply. The chosen method is to construct a model

of an intertidal transect, including the minimum set of processes needed for the comparison to be made. Model conditions can then be varied to compare responses under various biotic and physical forcings. The model uses sediment erosion functions, which incorporate bioturbation effects, within an advective model of sediment transport. Net erosion and deposition over a tidal cycle is then predicted over a one-dimensional shore-normal transect. The relative importance of biotic and physical forcing to the evolution of the bed can only be assessed when erosion and deposition effects are integrated under realistic tidal velocities. Previous models have not directly compared biotic effects with abiotic effects on intertidal sediment transport.

Intertidal areas have frequently been modeled as part of two-dimensional or three-dimensional models of whole estuaries (Cheng et al. 1993; le Hir et al. 2000). These models are larger and more complex than is needed for our purpose here, which is more an experimental investigation into combining processes rather than a predictive model for a particular area. One-dimensional models of cross-shore transects have been used by Woolnough et al. (1995) for studying morphological evolution of salt marshes. Goodwin et al. (1992) used “methods of characteristics” to model propagation of the tidal surface wave across the intertidal zone. Wood et al. (1998) modeled a one-dimensional transect across Spurn Bight using simplified equations, and the results compared favorably with current meter observations at about midtide level. Friedrichs and Aubrey (1996) examined the velocities over a uniformly sloping bed due to volume conservation of a flooding and drying tidal flow. Recently, le Hir et al. (2000) reaffirmed the suitability of assuming a horizontal water surface across tidal flats where the long-shore flow is small, and Roberts et al. (2000) confirm that cross-shore flows dominate at Skeffling.

Many experiments and observations have confirmed that

¹ Corresponding author (r.wood@pml.ac.uk).

Acknowledgments

This work was supported under the Emphasys Phase I research program (funded by MAFF and the EA), the DEFRA-funded BIOSSED program (contract AE0259), and by the NERC Land-Ocean Interaction Study program. The authors would like to thank two anonymous reviewers for useful comments.

benthic animals can affect sediment erosion and deposition. Graf and Rosenberg (1997) review the direct (e.g., sediment disturbance by siphon feeding, production of large pseudofeces) and indirect (e.g. effects on flow speed and effects of mucus on particle cohesiveness) mechanisms of bioresuspension and biodeposition. They conclude that erosional or depositional fluxes can be more than doubled by benthic biota. Biopolymers exuded by microphytobenthos have been observed to increase sediment stability (de Brouwer et al. 2000) and increase erosion thresholds (Amos et al. 1998; Austen et al. 1999; Widdows et al. 2000*a,b*). Bioturbation by *Macoma balthica* has been studied by Widdows et al. (1998*b*). Flume experiments within the laboratory and in the field showed significant increases in erosion rates in relation to *Macoma* densities. Clearly, the erosional behavior of a mudflat will be affected by spatial and temporal changes in the densities of a range of key species acting as biostabilizers and biodestabilizers. However, for the purposes of this study, which is an assessment of the scope of biological influence on sediment movement, only the bioturbation by *Macoma* and biostabilization by diatoms will be considered.

Model description

The model combines a simple one-dimensional onshore-offshore model of water movement with a semiempirical model of cohesive sediment erosion and deposition. The model transect is taken as representative of a section of estuarine shore that is uniform in the longshore direction. The population densities of *Macoma* and microphytobenthos are specified along the transect.

Depth-averaged current speed—The sea surface is taken to be flat across the model extent. Time-varying sea surface elevation is supplied at the offshore boundary. Depth-averaged velocities are calculated along the transect using volume conservation (as described in Wood et al. 1998)

$$\frac{\partial \eta}{\partial t} + \frac{\partial}{\partial x}(u[\eta - H]) = 0$$

where η = sea surface elevation relative to chart datum, H = height of bed relative to chart datum, and u = current speed in the x direction (offshore). The drying height in the model is set to 5 cm.

Sediment transport—The sediment transport is calculated using an advection equation for suspended matter, with erosion and deposition terms

$$\frac{\partial C}{\partial t} + \frac{\partial}{\partial x}(uC) = \frac{(E - D)}{(\eta - H)}$$

where C = suspended sediment concentration, E = erosion rate, and D = deposition rate. Suspended sediment can be imported or exported through the open, offshore boundary of the model and can be eroded from the bed or deposited onto it. The suspended sediment is assumed to be well mixed throughout the water column.

Erosion rate—The depth-averaged current speed is used to calculate the speed at 10 cm above the bed (using an

estimated value for bed roughness, *see below*). This near-bed current speed is then used in the erosion formulation to give erosion rate. Erosion rate is also dependent on the density of *Macoma* in the bed sediment. Willows et al. (1998) used flume data to form a semiempirical model formulation for behavior of suspended sediment within the flume, dependent on water velocity and *Macoma* density. When exposed to a constant velocity that exceeds the critical erosion velocity, increasing the density of *Macoma* leads to larger amounts of sediment being eroded. Increasing *Macoma* density further has a progressively smaller effect until an asymptote is approached. This corresponds to the siphoning ranges of *Macoma* individuals covering the whole surface of the sediment. Comparison with field data from the Skeffling transect in the Humber show that the same functional form fits field data with similar parameter values.

Current speed and *Macoma* density (number of 7 mm or longer individuals m^{-2}) determine the sediment erosion rate, E ,

$$E = k(\text{mxsed}(n, u_{10\text{cm}}) - \text{erodsed})$$

$$\text{if } |u_{10\text{cm}}| > u_{\text{crit}_e} \quad \text{and} \quad \text{mxsed}(n, u_{10\text{cm}}) > \text{erodsed},$$

$$\text{otherwise } E = 0$$

where $u_{10\text{cm}}$ is the model current speed estimated at 10 cm above the bed, $\text{mxsed}(n, u_{10\text{cm}}, x)$ is the maximum erodable sediment per unit area for *Macoma* density n and current speed u , $\text{erodsed}(x)$ is the amount of sediment eroded since the erosion commenced, u_{crit_e} is critical erosion speed, and parameters k and those in mxsed are experimentally determined. The functions mxsed and erodsed are described in Willows et al. (1998), along with the parameters from Skeffling field experiments that are used here. The erosion formulation (in which erosion rate varies with mass of sediment already eroded) is equivalent to an erosion rate that varies with depth of sediment eroded.

Current speed at 10 cm above bottom—The erosion function is in terms of current speeds at 10 cm above the bed because this is the height at which speeds are measured in the annular flume. The relationship between current velocity and estimated bed shear stress is given in Widdows et al. (1998*a*). To estimate current speed within the model at 10 cm above the bed, a factor is used, based on the following relations. A logarithmic velocity profile is assumed

$$u(z) = \frac{u_*}{\kappa} \ln\left(\frac{z}{z_0}\right)$$

where $u(z)$ = current speed at height z above bed level, κ = von Karman's constant, z_0 = roughness length, and u_* = friction velocity.

This can be integrated over depth to give u_* in terms of depth-averaged velocity, \bar{u} ,

$$u_* = \frac{H\kappa\bar{u}}{\left\{ H \ln\left(\frac{H}{z_0}\right) - H - z_0 \right\}}$$

This can then be used in the velocity profile equation to find $u(0.1)$,

$$u(0.1) = \ln\left(\frac{0.1}{z_0}\right) \frac{H\bar{u}}{\left\{H \ln\left(\frac{H}{z_0}\right) - H - z_0\right\}} = f_1 \bar{u}$$

Appropriate roughness lengths for mud or muddy sand are between 0.0002 m and 0.0007 m (Dyer 1986). For values of H between 2 m and 8 m, and taking $\kappa = 0.4$, then f_1 varies between 0.76 and 0.59. In the model, the factor f_1 is approximated as 0.7.

Critical erosion threshold—The threshold speed at which erosion starts is taken as a linear function of surface chlorophyll a (Chl a) concentration. This is based on observations in the Westerschelde (Widdows et al. 2000a) and supported by the experimental results of Sutherland et al. (1998).

The equation is

$$u_{\text{crit}_e} = 0.01(0.4026 \text{ Chl} + 15.934)$$

where Chl = chlorophyll a concentration in the surface sediment ($\mu\text{g g}^{-1}$ dry weight of sediment, measured in 1 cm deep core), and u_{crit_e} is in m s^{-1} .

During the field deployments of the flume at Skeffling, similar critical erosion velocities from 0.15 to 0.31 m s^{-1} were observed (Widdows et al. 1998a).

Sediment deposition—Sediment deposition rate is calculated using the basic equation of Krone (1962) with a single settling velocity and critical deposition speed based on experimental data from Amos et al. (1998) and Widdows et al. (1998a)

$$D = w_s C \left(1 - \frac{u_{10\text{cm}}^2}{u_{\text{crit}_d}^2}\right) \quad \text{if } u_{10\text{cm}} < u_{\text{crit}_d}$$

where w_s is settling velocity ($w_s = 0.5 \text{ mm s}^{-1}$), $u_{10\text{cm}}$ is speed 10 cm above the bed, and u_{crit_d} is critical deposition speed ($u_{\text{crit}_d} = 0.12 \text{ m s}^{-1}$).

The choice of fall velocity was based on flume observations of decreases in suspended particulate matter after current speeds were reduced below the deposition threshold velocity.

Output variables and model parameters—The model is constructed within the ECoS modeling system (Gorley and Harris 1998), allowing easy change of most of the process equations. Model runs start from rest, with no suspended sediment and with the tidal state at low water. Sea surface elevation and suspended sediment concentration are specified at the offshore boundary. Output variables that are produced at every time step are current speed, suspended sediment concentration, and net sediment mass eroded or deposited within each segment in the transect. The model runs for single tidal cycles. At the end of a tidal cycle, the model produces a profile of net erosion and deposition of sediment (mass per unit area). Model runs are made for a variety of boundary conditions and biota distributions. Results are then summed appropriately to give budgets of sediment movement due to these processes for sequences of tides. The time step for the model is 60 s. The model has

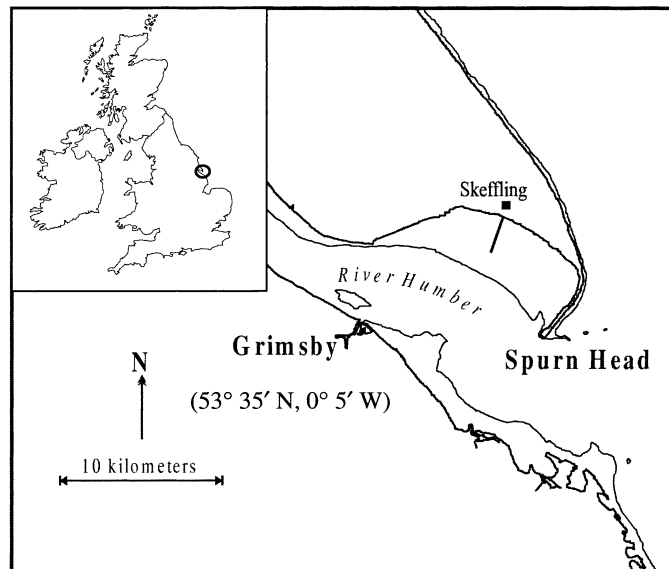


Fig. 1. Location of modeled transect at Skeffling in the outer Humber estuary, England, showing coastline and level of chart datum (approximately the level of lowest astronomical tide).

also been run with time steps of 30 s and 15 s, and there was no significant change in the results. Spatial segments are 35 m in length. The model uses centered differencing in space, and forward differencing in time. Results are stored every 600 s, and shown in the subsequent plots.

Model parameterization

This study is concerned with investigating simplified biotic-physical systems, rather than accurately reproducing conditions in a particular estuary. However, input parameters for the model have been based on a transect for which present-day and historical data on bed elevation does exist. The transect is on the Skeffling mudflats in Spurn Bight on the north shore of the outer Humber estuary, England (Fig. 1). This transect extends from the shoreline embankment to 3.5 km offshore (where the bed is below mean low water neaps level). This intertidal area is wide and flat, and so velocity is expected to be predominantly cross shore (Dyer 1998). Bed heights have been obtained from profiles measured during the Littoral Investigation of Sediment Properties (LISP) experiment (Black 1998). Ideally, the cross-shore bathymetry should be averaged over several kilometers of shoreline. To approach this, the bathymetry is smoothed so that cross-cutting channels are not included.

The bathymetry for the Skeffling model is shown in Fig. 2. Modeled currents are fastest near midtide level at the time of flooding and drying (when the rate of sea surface rise is greatest), as well as at flooding and drying of the flattest part of the profile (about 750–1,000 m offshore). The spatial distributions of *Macoma* and Chl a in the model are also shown.

The variation of *Macoma* density along the transect is calculated using the following formula (McGrorty and Yates pers. comm. 1999) based on bed height and bed sediment grain size.

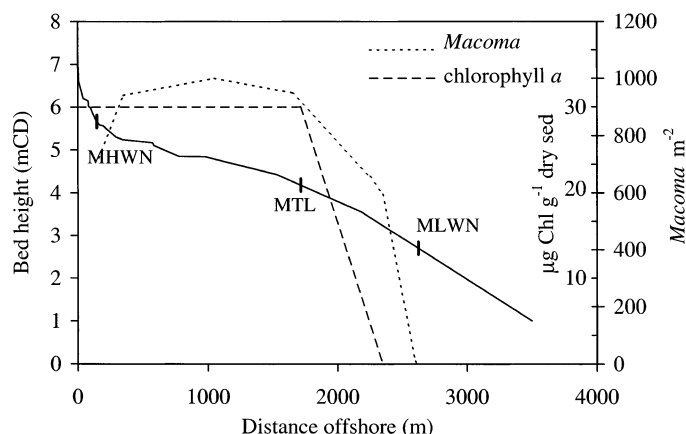


Fig. 2. Bathymetry for the Skeffling transect, with locations of mean high water neaps (MHWN), midtide level (MTL), and mean low water neaps (MLWN) marked. Height given in meters above chart datum (mCD). Spatial profiles of density of *Macoma balthica* individuals and surface Chl *a* concentration are also shown.

$$n = c \exp(A)$$

$$A = 1.72 + 0.121p + 1.486h - 0.01345ph - 0.001009p^2 - 0.2459h^2$$

where n = *Macoma* density (number of individuals m^{-2}), c = scaling factor to give a chosen maximum density, p = percentage of fine material ($<63 \mu m$) in bed sediment, h = height of bed relative to ordnance datum Newlyn, U. K. The range of values used for c was based on observations by Widdows et al. (1998a, 2000b) in the Humber, and Beukema et al. (1998) in the Wadden Sea. This formula arises from a multiple regression of observed *Macoma* numbers against physical parameters using data from the Wash and Humber. For the Skeffling transect, this produces a simple unimodal variation of *Macoma* numbers down the shoreline, with a broad maximum centered around 1,000 m offshore, a rapid fall to low numbers as the sediment becomes sandy, and a reduction in numbers at the highest shore levels (as shown in Fig. 2).

Values for the surface sediment Chl *a* concentration (as related to the density of diatoms) were chosen based on observations by Amos et al. (1998) at Skeffling, by Underwood and Paterson (1993) in the Severn, and by Widdows et al. (2000a) in the Westerschelde. The distribution of diatoms down the shore was based on measurements by Amos et al. (1998) at Skeffling and on particle size variation down the shore.

Model results

The net mass of bed sediment deposited or eroded at each grid cell during a single tidal cycle is taken as the model response. The main forcings within the model (tide height, bioturbator density, microphytobenthic chlorophyll concentration, and external sediment) have been varied individually to show the effect that each has on the response over a single tide. For investigation of longer term bed changes, results

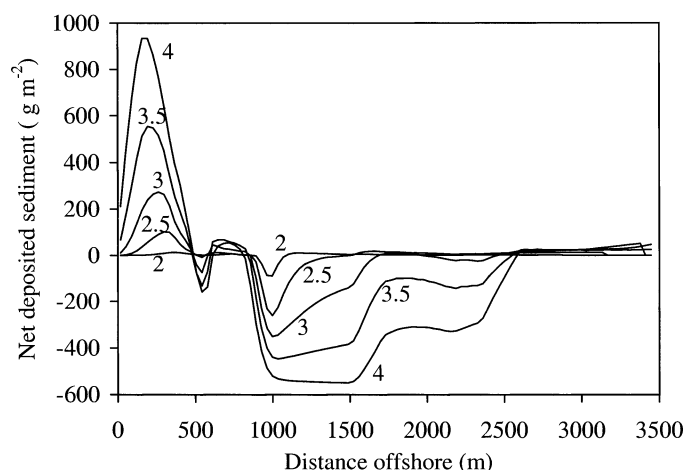


Fig. 3. Model results of net deposition of sediment during one tidal cycle for five different tidal amplitudes. Negative values correspond to erosion, and positive values correspond to accretion. Response lines are labeled with tidal amplitude (in m).

for 29 separate tidal cycles are then summed to approximate the response over two spring-neap cycles.

Effect of tide height—Figure 3 shows net erosion and deposition during tides of five different amplitudes. For these runs, the peak *Macoma* density is 1,000 individuals m^{-2} and the peak Chl *a* density is $30 \mu g g^{-1}$ dry surface sediment. Incoming water is set to have zero suspended particulate matter (SPM), so there is no external sediment supply for these runs. The intertidal erosion and up shore transport gives a strong peak of deposition in the high shore zone. These results, combined with those from other runs, show that the height, spread, and location of this peak are strongly dependent on the tide height, bed geometry of this zone, and deposition parameters used. There is large intertidal sediment transport at springs (4 m amplitude), but very little transport at neaps (2 m amplitude). Peak deposition reduces by a factor of 75 for a change in tidal amplitude from 4 m to 2 m. Peak erosion reduces by a factor of over six for the same tidal amplitude change, and the cross-shore extent of erosion reduces by a similar factor. An increase in tidal amplitude from 3 m to 4 m gives a greater than threefold change in maximum deposition. This shows that the higher tides will give a much greater contribution to the mass of intertidally transported sediment than the small to medium tides. This is consistent with measurements of tidally averaged SPM flux at Skeffling by Black (1998), which show net onshore flux at site B (585 m offshore) during spring tides and no significant transport during neap tides.

The mass of sediment that undergoes net transport has been summed over one tidal cycle and over the entire transect. This shows that for a 3 m tide, 90 kg of sediment per meter of longshore distance are transported shoreward and 79 kg of sediment per meter of longshore distance are exported from the model system. In reality, much of this may be expected to return as suspended load during the subsequent tide. For a 4 m tide, the mass of sediment transported

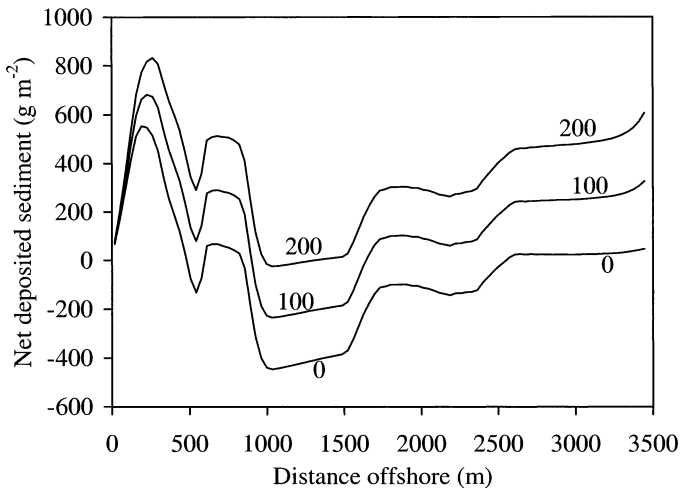


Fig. 4. Model results of net deposition of sediment during one tidal cycle for three different offshore suspended sediment concentrations. Response lines are labeled with offshore SPM concentration (in g m^{-3}).

up shore is 288 kg m^{-1} longshore, while the mass of sediment exported is 390 kg m^{-1} longshore.

Effect of changing external sediment—Figure 4 shows net deposition after one tide for three values of incoming suspended sediment concentration. For these runs, there is a maximum *Macoma* density of $100 \text{ individuals m}^{-2}$ and a maximum Chl *a* density of $30 \mu\text{g g}^{-1}$ dry sediment. The tidal amplitude is set to 3.5 m. External suspended sediment concentration is set to 0, 100, and 200 g m^{-3} , respectively. This is a reasonable range given that measured values of suspended solids in the Humber mouth vary from 20 to $1,000 \text{ g m}^{-3}$ (Gameson 1982). Sediment is deposited, using a constant fall velocity, while current velocity is below a deposition threshold. At lower shore locations, the results are dominated by the difference in external sediment supply. At higher shore levels the response lines are closer together, which shows that the deposition of intertidally transported sediment is outweighing the contribution from externally sourced sediment here. At middle shore levels, the intertidal erosion of the bed is being countered by deposition of sediment advected from the subtidal channel when external sediment supply is not zero. This shows that effects of intertidal sediment transport become more important at higher shore levels.

Effect of changing biota—Figure 5 shows net erosion and deposition after one 3.5 m spring tide for four different biota scenarios. There is no external sediment supply for these runs. High *Macoma* values tend to be associated with lower diatom values due to increased grazing pressure. Because of this, the high *Macoma* runs are given a lower maximum Chl *a* value than the low *Macoma* runs. The responses show the hydrodynamics determining the spatial pattern of erosion/accretion, with biota strongly influencing the magnitude. The response curves can be considered as forming two groups. The curves (H, L) and (H, H) have high numbers of bioturbators and show large midshore erosion and subsequent on-

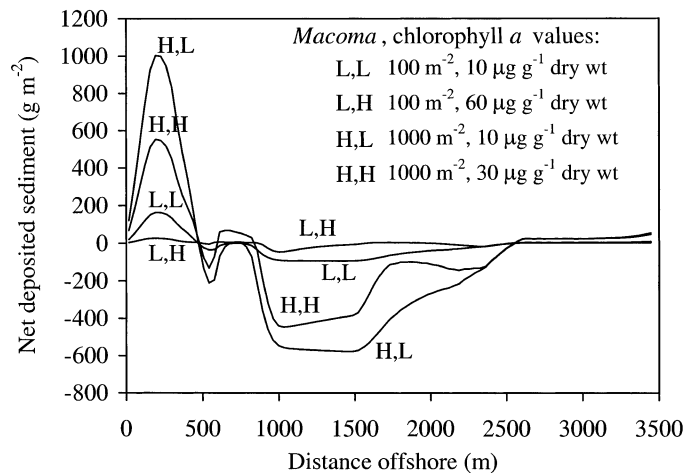


Fig. 5. Model results of net deposition of sediment during one tidal cycle for low *Macoma* + low Chl *a* (L, L); low *Macoma* + high Chl *a* (L, H); high *Macoma* + low Chl *a* (H, L); and high *Macoma* + high Chl *a* levels (H, H).

shore deposition, whereas the curves (L, H) and (L, L) have low numbers of bioturbators and show much smaller responses. Within these groups, the curves with higher chlorophyll (H, H and L, H) show reduced accretion and erosion compared to the lower chlorophyll runs (H, L and L, L). Increasing the *Macoma* density from 100 to $1,000 \text{ individuals m}^{-2}$ increases the erosion at 100 m offshore and increases the peak deposition by fivefold on the upper shore. Further increases in *Macoma* numbers would not significantly enhance the effect, since the erosion rate shows asymptotic behavior in the presence of higher *Macoma* densities (greater than $1,000 \text{ individuals m}^{-2}$). The *Macoma* density affects erosion rate, whereas diatom density affects critical erosion speed. So increasing diatom density can prevent erosion in parts of the transect where it previously occurred, whereas changing overall *Macoma* numbers influences the magnitude but not, primarily, the spatial distribution of erosion.

Month-long results—Model results show a strong spring-neap variation. Biota and external sediment supply are expected to vary less rapidly. Therefore, to show cumulative effects over two spring-neap cycles, results for individual tides are summed over 29 d, and converted to depth of net accretion or erosion. An appropriate sequence of tide heights is taken from Admiralty Tide Tables (1998). Model responses for all the tides during 1–29 November 1998 have been summed, using several biota populations. Areas that are below the mean low water spring (MLWS) level are not shown. For comparison, one set of runs is made with no intertidal erosion. By use of observed values of wet sediment density ($1,325 \text{ kg m}^{-3}$) and dry sediment density ($2,650 \text{ kg m}^{-3}$), the net deposition has been converted to depth of sediment accretion (Fig. 6). With no intertidal erosion allowed, the amount of deposition increases smoothly with offshore distance. The change of deposition with distance is steepest at the highest shore levels. Using a low density of bioturbators ($100 \text{ Macoma m}^{-2}$, and a chlorophyll value of $20 \mu\text{g g}^{-1}$

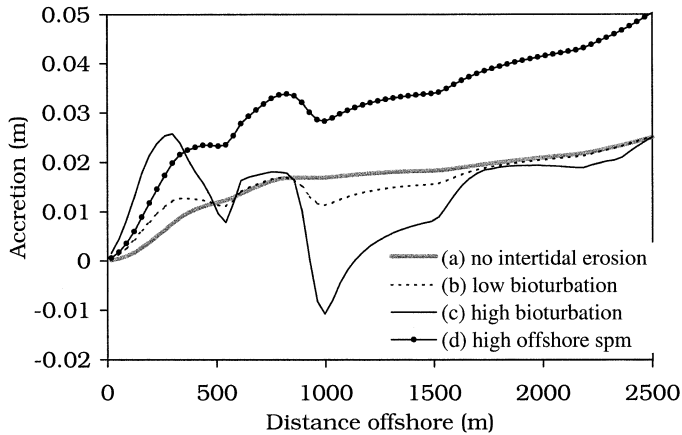


Fig. 6. Model results of accretion of sediment during 1–29 Nov 1998 with (a) no intertidal erosion and moderate offshore suspended sediment (100 g m^{-3}), (b) low *Macoma* ($100 \text{ individuals m}^{-2}$) and moderate offshore sediment supply (100 g m^{-3}) and surface Chl *a* concentration of $20 \mu\text{g g}^{-1}$ dry sediment, (c) high *Macoma* ($1,000 \text{ individuals m}^{-2}$) and moderate offshore sediment supply (100 g m^{-3}) and surface Chl *a* concentration of $30 \mu\text{g g}^{-1}$ dry sediment, (d) low *Macoma* ($100 \text{ individuals m}^{-2}$) and high offshore sediment supply (200 g m^{-3}) and surface Chl *a* concentration of $20 \mu\text{g g}^{-1}$ dry sediment.

dry sediment) changes the response by reducing deposition at the midshore range and increasing deposition at the high shore. High bioturbation ($1,000 \text{ Macoma m}^{-2}$, and a Chl *a* value of $30 \mu\text{g g}^{-1}$ dry sediment) has a large effect on the response, giving a large peak in deposition below the mean high water neap (MHWN) mark and a broad band of erosion and reduced deposition around midtide level. Comparing the responses to high bioturbation with 100 g m^{-3} external sediment and low bioturbation with 200 g m^{-3} offshore sediment supply shows that the high-shore deposition associated with a high density of *Macoma* can exceed that given by a large offshore sediment supply. Integrating over a month has lowered and broadened the deposition peak.

Model validation

Ideally, the results of the model should be compared to observations of erosion and deposition over an intertidal flat for individual tides during periods of low winds. However, there are very few data of this sort available. The model has been built up using parameterizations from flume experiments that have been validated against field experiments. The performance of the velocity model has been validated against field data in Wood et al. (1998). In Figs. 7 and 8, the model results for suspended particulate matter are compared against observed concentrations at two locations along the transect. The advantages of using SPM to validate the model are that it is a more easily measurable quantity than bed level and more measurements are available and that it is an advected quantity with an extensive source, so it naturally integrates spatially. It is likely to display smoother behavior that is more comparable to an idealized one-dimensional model. Figure 7 shows modeled and observed depth-averaged SPM at site B (585 m offshore) for the af-

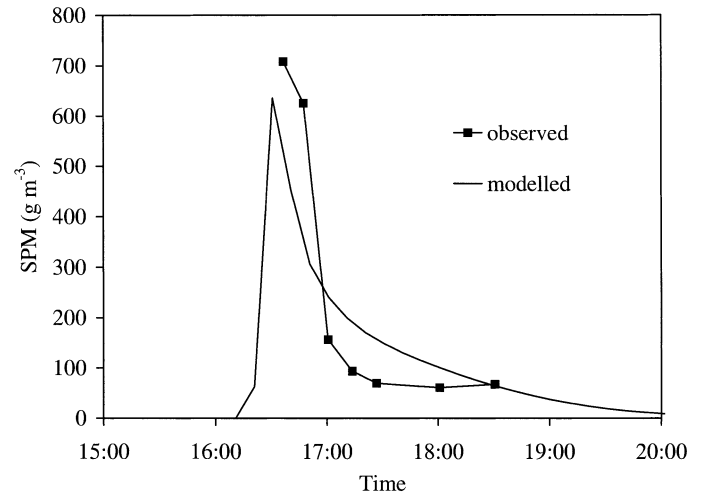


Fig. 7. Observed and modeled suspended particulate matter (SPM) concentration at site B (585 m offshore). Observations from unpublished data of M. Christie (pers. comm. 2000).

ternoon flood tide of 4 July 1997. The wind conditions were calm and the tidal range at Spurn was 5.2 m. The observations are taken from unpublished data (M. Christie 2000 pers. comm.) from the MAST 3 INTRMUD project, contract number MAS3-CT-95-0022. The model had a maximum *Macoma* density of $1,000 \text{ individuals m}^{-2}$, a maximum Chl *a* concentration of $10 \mu\text{g g}^{-1}$ dry sediment, and an external suspended sediment concentration of 200 g m^{-3} . The model reproduces the initial peak in SPM as the area floods, followed by reduction in SPM due to settling around high water. The model shows more settling than the observations because model current speeds fall to zero at high tide, whereas in reality there is a small longshore component of flow around high tide.

Figure 8 shows modeled and observed SPM at site D (about 2,200 m offshore) for the same tide. Observed values were taken from Christie et al. (1999). A broad low peak in

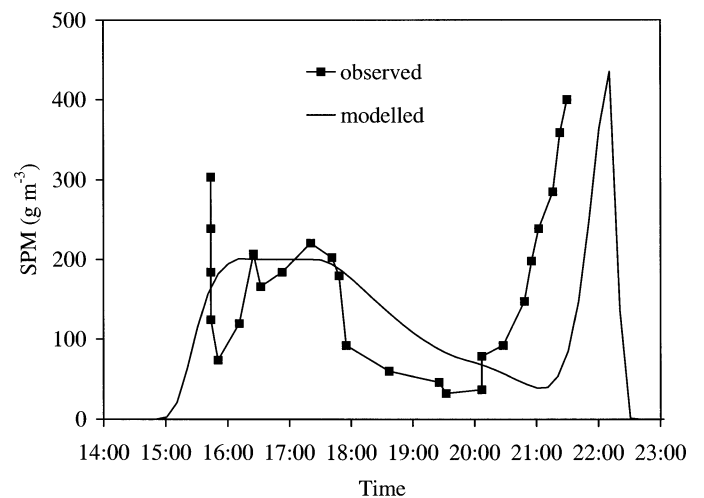


Fig. 8. Observed and modeled suspended particulate matter (SPM) concentration at site D (2,200 m offshore). Observations from Christie et al. (1999).

SPM is seen during the flood phase in both the observations and model results. This is related to the concentration of sediment being advected into the system from offshore. During the ebb, the observations show a sharp peak in SPM as water depth becomes shallow and ebb speed increases. This is reproduced in the model. These comparisons indicate that on a tidal timescale the model is producing the main observed features of SPM behavior.

A pattern of high-shore accretion and midshore erosion at Skeffling has also been inferred by Andersen et al. (2000) based on observations of ^{210}Pb and ^{137}Cs in sediment cores. Vertical profiles of ^{210}Pb concentration from a sample at site A (50 m offshore) implied accretion of about 8 mm yr^{-1} . Profiles from sites B (600 m offshore) and C (1,500 m offshore) were not consistent with accretion, but implied erosion. This is in agreement with the pattern shown by the model (in Fig. 6, line c, for example). At site A the model shows accretion; at site B it shows small erosion; and at site C the model shows larger erosion.

There are few direct observations of sediment erosion and deposition on a tidal timescale. However, Brown (1998) observed up to $650 \text{ g dry weight m}^{-2}$ of sediment deposited on the upper salt marsh during two tidal cycles. A model run with a tidal amplitude of 4 m, zero external sediment supply, maximum *Macoma* density of $1,000 \text{ individuals m}^{-2}$, and Chl *a* concentration of $30 \mu\text{g g}^{-1}$ dry sediment gives similar magnitudes of $210 \text{ g dry weight m}^{-2}$ of sediment deposition over a single tide at 15 m offshore.

Discussion

Within this model, the fundamental forcing is the tidal current. It is tidal current speed that provides energy to cause intertidal sediment transport. The biota affect the erosion response to any particular tidal forcing. The magnitude of biological and physical effects on intertidal accretion and erosion during calm conditions can be assessed by comparing the response to changes in physical variables (tide height, external SPM concentration) and biological variables (*Macoma* density, diatom density—as indicated by Chl *a* concentration). The utility of the model lies partly in the ability to separate biological and physical processes, which cannot be separated by field observations of integrated quantities such as SPM.

The pattern of intertidal erosion is sensitive to the bathymetry, with greatest erosion occurring over flatter sections of shore (where peak current velocities are higher). Comparing results for different tidal ranges shows that there is little transport during neap tides, so the influence of individual tides is highly biased toward the larger tidal ranges. Increasing the external sediment supply gives greater deposition on the lower intertidal area, but the effect diminishes as the shoreline is approached (and inundation time decreases). Altering the density of bioturbating clams from a low to a high value (consistent with observed interannual variations; Widdows et al. 2000a,b) can increase the peak value of deposition on the higher shore by a factor of five. Increasing the Chl *a* density (related to the presence of microphytobenthos) can reduce the high-shore deposition peak by

a factor of two. These results have been computed for a wide tidal flat in a macrotidal estuary (Spurn Bight, Humber estuary, UK). The qualitative aspects of the comparison between biotic and purely physical effects are generally applicable to this type of estuarine situation, i.e., sheltered extensive intertidal areas with a large tidal range. The results show that biota can have a significant effect on sediment redistribution within the intertidal zone. This is important for the morphological evolution of intertidal areas.

In a regime of climate change, where changes in summer temperatures and cloud cover will influence diatom growth and changes in patterns of mild and severe winters will influence *Macoma* populations, this work shows that biota have an important role in determining the intertidal sediment budget. Diatom numbers follow a seasonal pattern, with higher densities in spring and (sometimes) autumn. *Macoma* numbers show greater interannual than seasonal variation, with high recruitment years tending to follow cold winters (Beukema et al. 1998; Widdows et al. 2000a,b). In this model, high *Macoma* populations will destabilize the midshore sediment, which increases deposition at high shore levels. Further observations of bed-level change and biota are required to establish the statistical significance of biotic effects on a large spatial scale.

There is plentiful supply of external sediment to the lower intertidal zone, which is covered by most tides, and yet the observed accretion becomes much higher near and within the salt marsh zone. Intertidal erosion removes sediment from midshore levels, where the deposition from external supply is plentiful, and redistributes it on the higher shore.

Intertidal transport gives a mechanism for external sediment to be shifted up shore on spring tides. At midtide levels, the erosion on the flood and deposition of sediment advected in from offshore can give large sediment transport without much local change in bed level. The magnitude of the intertidal transport will be affected by biota, which themselves vary with season and year. Physical characteristics like bed height and size of bed sediment particles are not sufficient to parameterize biotic effects because of seasonal and interannual variability of biota populations.

The model results show a rate of bed-level change that is higher than that observed over longer timescales (Wood 2000). However, Allen and Duffy (1998) noted that at upper intertidal points in the Severn estuary, rates of bed-level change over 2 yr were five times smaller than monthly rates of change. This confirms the idea that morphological change of intertidal areas is the net result of competing accretionary and erosionary processes, with different processes dominant at different times. It appears that changes over long timescales are the (small) balance of larger changes occurring over shorter timescales.

The model presented in this paper clearly represents a simplified system, which does not produce all major terms in the sediment transport budget. A near-bed wave orbital velocity can also be added, or velocity could be modified to take account of wave-current interaction, this would then allow consideration of periods of windy conditions. A natural population of particles, including the development of flocs, would have a range of fall velocities, which may alter the pattern of high-shore deposition. The sediment transport

behavior for a sequence of tides is dependent on the reestablishment of vertical erodability structure within the sediment column during exposure or inundation. This will be affected by compaction and consolidation processes as well as biotic disturbance. Observations are needed to determine suitable choices for specific situations. Temporal variation in external suspended sediment and the effects of surges and cycles longer than the spring-neap cycle on tidal height will also affect the long-term sediment transport budget. Furthermore, bathymetric changes resulting from the erosion and deposition will feed back to affect currents and subsequent erosion patterns. Further observations of bed-level change and biota are required to establish the statistical significance of biotic effects on a large spatial scale.

References

- ADMIRALTY TIDE TABLES, VOL. 1. 1998. U.K. Hydrographic Office.
- ALLEN, J. R. L., AND M. J. DUFFY. 1998. Medium-term sedimentation on high intertidal mudflats and salt marshes in the Severn Estuary, SW Britain: The role of wind and tide. *Mar. Geol.* **150**: 1–27.
- AMOS, C. L., M. BRYLINSKY, T. F. SUTHERLAND, D. O'BRIEN, S. LEE, AND A. CRAMP. 1998. The stability of a mudflat in the Humber estuary, South Yorkshire, UK. *In* K. S. Black, D. M. Paterson, and A. Cramp [eds.], *Sedimentary processes in the intertidal zone*. *Geol. Soc. Lond. Spec. Publ.* **139**: 25–44.
- ANDERSEN, T. J., O. A. MIKKELSEN, A. L. MOLLER, AND M. PEJRUP. 2000. Deposition and mixing depths on some European intertidal mudflats based on Pb-210 and Cs-137 activities. *Cont. Shelf Res.* **20**: 1569–1591.
- AUSTEN, I., T. J. ANDERSEN, AND K. EDELVANG. 1999. The influence of benthic diatoms and invertebrates on the erodability of an intertidal mud flat. *Estuar. Coast. Shelf Sci.* **49**: 99–111.
- BEUKEMA, J. J., P. J. C. HONKOOP, AND R. DEKKER. 1998. Recruitment in *macoma balthica* after mild and cold winters and its possible control by egg production and shrimp predation. *Hydrobiology* **375/376**: 23–34.
- BLACK, K. S. 1998. Suspended sediment dynamics and bed erosion in the high shore mudflat region of the Humber Estuary, UK. *Mar. Pollut. Bull.* **37**: 122–133.
- BROWN, S. L. 1998. Sedimentation on a Humber saltmarsh. *In* K. S. Black, D. M. Paterson, and A. Cramp [eds.], *Sedimentary processes in the intertidal zone*. *Geol. Soc. Lond. Spec. Publ.* **139**: 69–84.
- CHENG, R. T., V. CASULLI, AND J. W. GARTNER. 1993. Tidal, residual, intertidal mudflat (TRIM) model and its applications to San Francisco Bay, California. *Estuar. Coast. Shelf Sci.* **36**: 235–280.
- CHRISTIE, M. C., K. R. DYER, AND P. TURNER. 1999. Sediment flux and bed level measurements from a macrotidal mudflat. *Estuar. Coast. Shelf Sci.* **49**: 667–688.
- DE BROUWER, J. F. C., S. BJELIC, E.M.G.T. DE DECKERE, AND L. J. STAL. 2000. Interplay between biology and sedimentology in a mudflat (Biezelingse Ham, Westerschelde, The Netherlands). *Cont. Shelf Res.* **20**: 1159–1177.
- DYER, K. R. 1986. Coastal and estuarine sediment dynamics. Wiley.
- . 1998. The typology of intertidal mudflats. *In* K. S. Black, D. M. Paterson, and A. Cramp [eds.], *Sedimentary processes in the intertidal zone*. *Geol. Soc. Lond. Spec. Publ.* **139**: 11–24.
- FRIEDRICH, C. T., AND D. G. AUBREY. 1996. Uniform bottom shear stress and equilibrium hypsometry of intertidal flats. *In* C. Pantiaratchi [ed.], *Mixing in estuaries and coastal seas, coastal and estuarine studies*. *Am. Geophys. Union* **50**: 405–429.
- GAMESON, A. L. H. 1982. Physical characteristics, p. 5–14. *In* A. L. H. Gameson [ed.], *The quality of the Humber Estuary*. Yorkshire Water Authority.
- GOODWIN, P., J. LEWANDOWSKI, AND R. J. SOBEY. 1992. Hydrodynamic simulation of small-scale tidal wetlands, p. 149–161. *In* R. A. Falconer, K. Shiono, and R. G. S. Matthews [eds.], *Hydraulic and environmental modelling: Estuarine and river waters*. Ashgate.
- GORLEY, R. N., AND J. R. W. HARRIS. 1998. ECoS3 user guide. Plymouth Marine Laboratory, Natural Environment Research Council.
- GRAF, G., AND R. ROSENBERG. 1997. Bioresuspension and biodeposition: A review. *J. Mar. Syst.* **11**: 269–278.
- KRONE, R. B. 1962. Flume studies of the transport of sediment in estuarial shoaling processes. University of California, Berkeley, Hydraulics Engineering Laboratory and Saint Engineering Laboratory.
- LE HIR, P., W. ROBERTS, O. CAZAILLET, M. CHRISTIE, P. BASSOULET, AND C. BACHER. 2000. Characterization of intertidal flat hydrodynamics. *Cont. Shelf Res.* **20**: 1433–1460.
- ROBERTS, W., P. LE HIR, AND R. J. S. WHITEHOUSE. 2000. Investigation using simple mathematical models of the effect of tidal currents and waves on the profile shape of intertidal mudflats. *Cont. Shelf Res.* **20**: 1079–1097.
- SUTHERLAND, T. F., C. L. AMOS, AND J. GRANT. 1998. The effect of buoyant biofilms on the erodability of sublittoral sediments of a temperate macrotidal estuary. *Limnol. Oceanogr.* **43**: 225–235.
- UNDERWOOD, G. J. C., AND D. M. PATERSON. 1993. Seasonal changes in diatom biomass, sediment stability and biogenic stabilization in the Severn Estuary. *J. Mar. Biol. Ass.* **73**: 871–887.
- WIDDOWS, J., M. D. BRINSLEY, AND M. ELLIOTT. 1998a. Use of an *in situ* flume to quantify particle flux (biodeposition rates and sediment erosion) for an intertidal mudflat in relation to changes in current velocity and benthic macrofauna. *In* K. S. Black, D. M. Paterson, and A. Cramp [eds.], *Sedimentary processes in the intertidal zone*. *Geol. Soc. Lond. Spec. Publ.* **139**: 85–98.
- , ———, P. N. SALKELD, AND M. ELLIOTT. 1998b. Use of annular flumes to determine the influence of current velocity and bivalves on material flux at the sediment-water interface. *Estuaries* **21**: 552–559.
- , ———, ———, AND C. LUCAS. 2000a. Influence of biota on spatial and temporal variation in sediment erodability and material flux on a tidal flat (Westerschelde, The Netherlands). *Mar. Ecol. Prog. Ser.* **194**: 23–27.
- , S. BROWN, M. D. BRINSLEY, P. N. SALKELD, AND M. ELLIOTT. 2000b. Temporal changes in intertidal sediment erodability: Influence of biological and climatic factors. *Cont. Shelf Res.* **20**: 1275–1290.
- WILLOWS, R. I., J. WIDDOWS, AND R. G. WOOD. 1998. Influence of an infaunal bivalve on the erosion of an intertidal cohesive sediment: A flume and modelling study. *Limnol. Oceanogr.* **43**: 1332–1343.
- WOOD, R. G. 2000. A model of biotically-induced sediment transport over an intertidal transect. *In* EMPHASYS Consortium. *Modelling estuary morphology and process*. Report TR 111. HR Wallingford, UK. 43–54.
- , K. S. BLACK, AND C. F. JAGO. 1998. Measurements and preliminary modelling of current velocity over an intertidal mudflat, Humber estuary, UK. *In* K. S. Black, D. M. Paterson, and A. Cramp [eds.], *Sedimentary processes in the intertidal zone*. *Geol. Soc. Lond. Spec. Publ.* **139**: 167–176.
- WOOLNOUGH, S. J., J. R. L. ALLEN, AND W. L. WOOD. 1995. An exploratory numerical model of sediment deposition over tidal salt marshes. *Estuar. Coast. Shelf Sci.* **41**: 515–543.

Received: 19 March 2001

Accepted: 17 December 2001

Amended: 4 February 2002